Structural Phase Transition and Electrical Conductivity of the Perovskite $CH_3NH_3Sn_{1-x}Pb_xBr_3$ and $CsSnBr_3$

Koji YAMADA,* Hiroshi KAWAGUCHI, Takashi MATSUI,
Tsutomu OKUDA, and Sumio ICHIBA
Department of Chemistry, Faculty of Science, Hiroshima University,
Higashisenda-machi, Naka-ku, Hiroshima 730
(Received February 16, 1990)

A series of solid solutions, $CH_3NH_3Sn_{1-x}Pb_xBr_3$ (x=0—1), having cubic perovskite structures was obtained by solid-state reactions. The ^{119}Sn Mössbauer spectra for $x<0.4$, however, indicated that the tin environment was considerably distorted from a regular octahedron at 110 K. On the other hand, a single Lorentzian spectrum having a large isomer shift was observed for $x>0.7$, suggesting the presence of a regular $SnBr_6$ octahedra in the perovskite $CH_3NH_3PbBr_3$ matrix. The high electrical conductivity of the perovskite $CsSnBr_3$ drastically decreased upon the replacement of the cation by CH_3NH_3 and the central metal by Pb. This behavior suggests that both the infinite linear chain (–Br–Sn(Pb)–Br–) and its bond length have significant importance regarding electrical conductivity.

Structural studies of Sn(II), Pb(II), and Ge(II) halides are interesting because of the existence of an s-electron lone pair. According to a VSEPR (Valence-shell electron pair repulsion) scheme, the structures of these molecules or anions are determined by the stereochemical activity of the lone pair.[1,2] However, the structural variety of the main group elements having an s-electron lone pair could not be fully understood systematically, especially for heavy p-block elements such as Sn(II), Sb(III), Pb(II), and Bi(III). In our previous papers, the structures of the SnX_3^- (X=halogen) anions were classified into four models by considering the geometry of the nearest neighbors around the tin atom.[3–5] Among these models, a regular octahedron, a square pyramid, and a trigonal pyramid were found in a series of $MSnX_3$ compounds. The structural diversity of SnX_3^- anions is due to the presence of two bonding scheme for the trans X–Sn–X bond, i.e. symmetric X–Sn–X and asymmetric X–Sn···X. The later is also described as a normal 2c-2e bond and an interanionic interaction. The former symmetric bond could be described as a typical three-center-four-electron bond (3c-4e) mainly using the p orbital of the central atom.[6–8] The Sn–X bond in the symmetric X–Sn–X bond has a higher ionic character than that of the normal Sn–X (2c-2e) bond, as was predicted by a simple MO model.[9] Therefore, in several compounds, such as $KSnBr_3 \cdot H_2O$ and $CsSnI_3$, the symmetric X–Sn–X bond deforms to X–Sn···X with decreasing temperature, while causing phase transitions.[3,5] Because of this characteristic deformation of the 3c-4e bond, many ferroelectric or piezoelectric phenomena are expected for compounds in this category.

In our structural study for a series of $MSnX_3$ compounds, the characteristic high electrical conductivity (of the order of 10^{2-3} S cm^{-1} and having a metallic temperature coefficient) has been observed for a crystal having a perovskite lattice, such as $CH_3NH_3SnI_3$ or $CsSnI_3$.[10] In these perovskite crystals, the trans I–Sn–I bonds are symmetric and form infinite chains along three orthogonal directions. In the present study, the structural deformations of $SnBr_3^-$ and $PbBr_3^-$ anions with decreasing temperature were investigated by means of the ^{81}Br NQR and ^{119}Sn Mössbauer effect. The electric property of the perovskite phases was also discussed.

Experimental

A series of solid solutions, $CH_3NH_3Sn_{1-x}Pb_xBr_3$ (x=0—1), was obtained by solid-state reactions. Stoichiometric amounts of CH_3NH_3Br, $SnBr_2$, and $PbBr_2$ were ground together using an agate mortar under a nitrogen atmosphere and heated at about 220—240 °C in an evacuated glass tube for several days. If necessary, the grinding and heating processes were repeated. $SnBr_2$ and $PbBr_2$ were purified by a Bridgman method and CH_3NH_3Br was recrystallized from methanol before use. A single crystal of $CsSnBr_3$ for the measurement of the electrical conductivity was obtained by a Bridgman method using stoichiometric amounts of CsBr and $SnBr_2$. Powder X-ray diffraction patterns were measured by a Rigaku Rad-B system using silicon powder as an internal standard. The NQR spectra were observed for end members with a pulsed spectrometer. The ^{81}Br and ^{79}Br resonance lines were assigned on the basis of the quadrupole moment ratio, $Q(^{79}Br)/Q(^{81}Br)$=1.1971. The electrical conductivity was measured using a single crystal of $CsSnBr_3$ and pressed powder pellets of $CH_3NH_3SnBr_3$ and $CH_3NH_3PbBr_3$ by a DC four-probe technique. The ^{119}Sn Mössbauer spectra were recorded at 110 and 293 K by means of a constant-acceleration-type spectrometer, using $Ca^{119m}SnO_3$ as a gamma-ray source. The velocity was calibrated with β-Sn and $BaSnO_3$.

Results and Discussion

Powder X-Ray Diffraction and DTA for Solid Solutions of $CH_3NH_3Sn_{1-x}Pb_xBr_3$. A series of solid solutions showed the characteristic X-ray powder patterns of the cubic perovskite, as can be seen in Fig. 1(A). The fine structures near (234) reflections are shown in Fig. 1(B) for three samples (x=0, 0.4, and 1) in order to prove the formation of the solid solution at

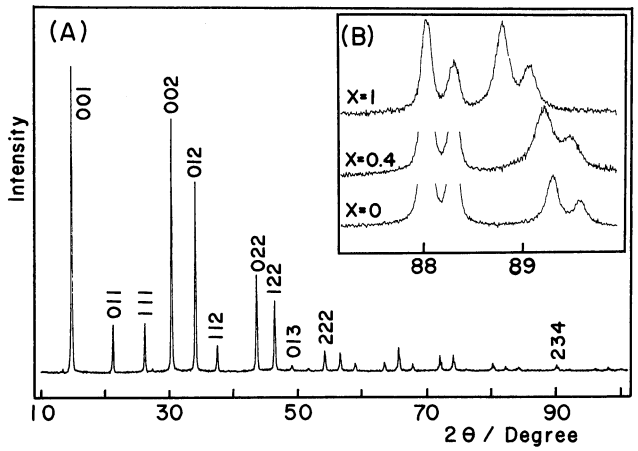

Fig. 1. Typical X-ray powder pattern for the solid solution having a perovskite structure. (A) $CH_3NH_3Sn_{0.9}Pb_{0.1}Br_3$; (B) Fine structures near (234) refractions for x=0, 0.4, and 1. The strong doublet at the left side corresponds to an internal standard of a silicon powder.

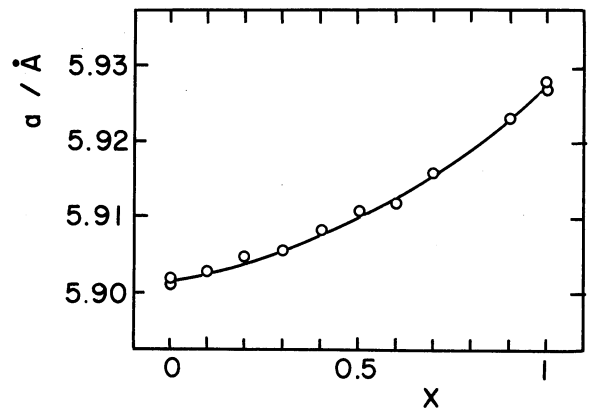

Fig. 2. Cubic lattice constants are plotted against x for a series of solid solutions, $CH_3NH_3Sn_{1-x}Pb_xBr_3$.

room temperature. Two pairs of $K_{\alpha 1}$ and $K_{\alpha 2}$ doublets near 88° and 89° correspond to reflections from a silicon (422) and a perovskite (234) plane, respectively. A slight broadening of the diffraction lines was observed for the solid solutions, compared to the end members, suggesting a slight inhomogeneity of the substitutional solid solution. Figure 2 shows plots of the cubic lattice constants against x. The lattice constant contracts slightly from that expected from the Vegard's law, this is consistent with the intense color in the intermediate solid solution. The DTA heating curves between 140 and 250 K for x=0, 0.2, 0.8, and 1 samples are shown in Fig. 3. The phase-transition temperatures, determined by averaging the heating and the cooling runs, were 150.9, 156.4, and 236.3 K for the Pb analogue and 184.2 and 229.3 K for the Sn analogue. These temperatures for the Pb analogue agreed well with those reported previously by means of DTA,[11] NQR,[12] and X-ray techniques.[13] In our

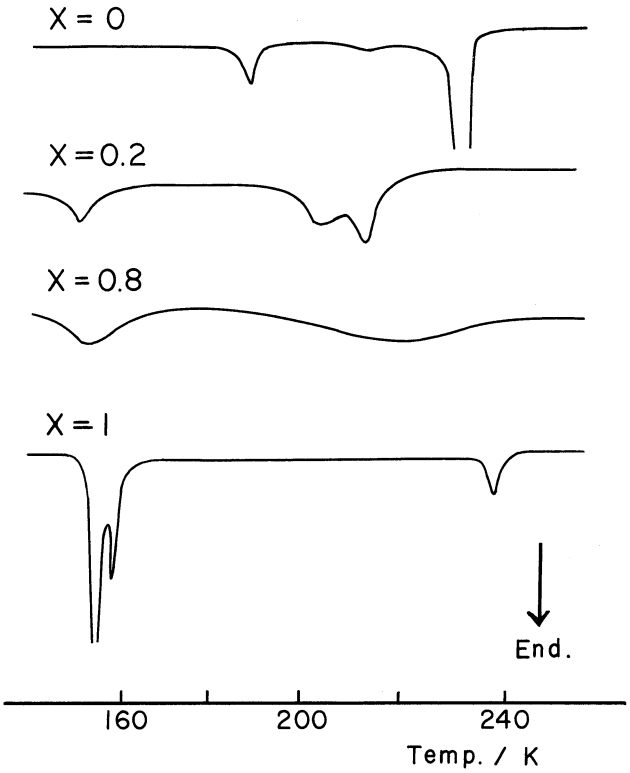

Fig. 3. DTA curves in the temperature range from 140 to 250 K for $CH_3NH_3Sn_{1-x}Pb_xBr_3$. Heating rate 2°C/min.

previous paper on $CH_3NH_3SnBr_3$, a drastic color change, from red to yellow, was observed at 229 K.[4] According to previous studies on $MSnBr_3$ compounds, intense colors such as red or black were observed only for crystals having perovskite lattices. Thus, the optical property of the perovskite family is supposed to arise from its characteristic band structure. The drastic color change of $CH_3NH_3SnBr_3$ suggests that the tin environment is considerably distored from a regular octahedron below 229 K, while destroying the symmetric linear chain.

With a deviation from the end members, all of the endothermic peaks became broader and their temperatures decreased. No sharp DTA peak was observed in the range $0.3<x<0.7$.

Structural Change of Anions by Means of ^{81}Br NQR. In our structural studies of $SnBr_3^-$ and SnI_3^- anions, drastic changes of the ^{81}Br, ^{127}I NQR spectra were often found upon increasing or decreasing the temperature.[3-5] In some favorable cases, the structural changes in these anions could be deduced from the NQR spectra below and above the phase transition. Figure 4 shows the temperature dependence of ^{81}Br NQR for $CH_3NH_3SnBr_3$ and $CH_3NH_3PbBr_3$. From the temperature dependence of the NQR spectra and also from the DTA curves, at least three and four phases were found to exist between 300 and 77 K for $CH_3NH_3SnBr_3$ and $CH_3NH_3PbBr_3$, respectively. The dotted lines indicate the phase-transition temperatures

Table 1. ^{81}Br NQR Frequencies for $CH_3NH_3SnBr_3$[a] and $CH_3NH_3PbBr_3$

Compounds	Phase	T/K	Frequency/MHz			Estimated error/MHz
$CH_3NH_3SnBr_3$	γ	77	74.95	72.83	71.93	0.05
			67.15	65.85	61.84	
	β	200	69.25	68.40	64.87	0.03
	α	300	65.725			0.01
$CH_3NH_3PbBr_3$	δ	77	61.667	58.234		0.005
	β	200	59.128	58.936		0.003
	α	300	58.844			0.002

a) Ref. 4.

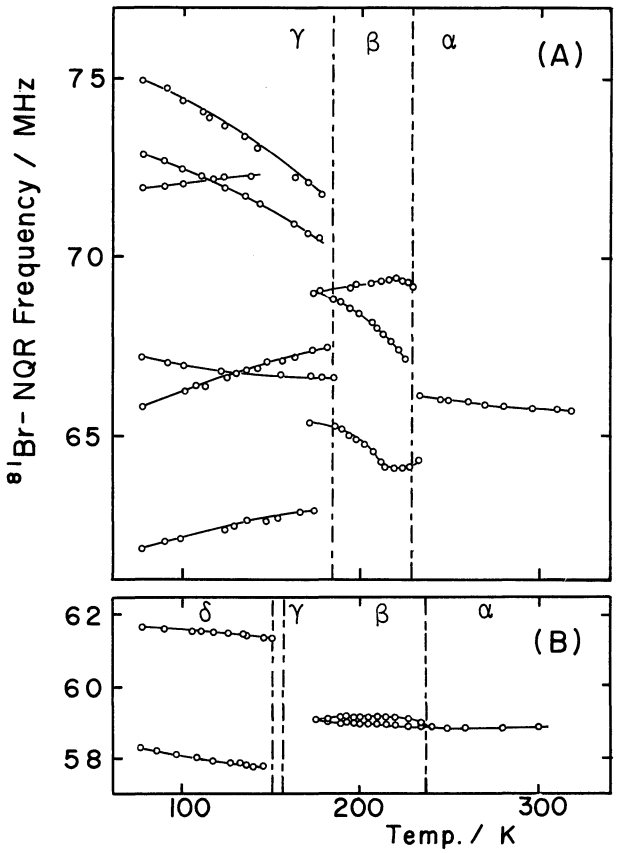

Fig. 4. ^{81}Br NQR temperature dependence for (A) $CH_3NH_3SnBr_3$ and (B) $CH_3NH_3PbBr_3$.

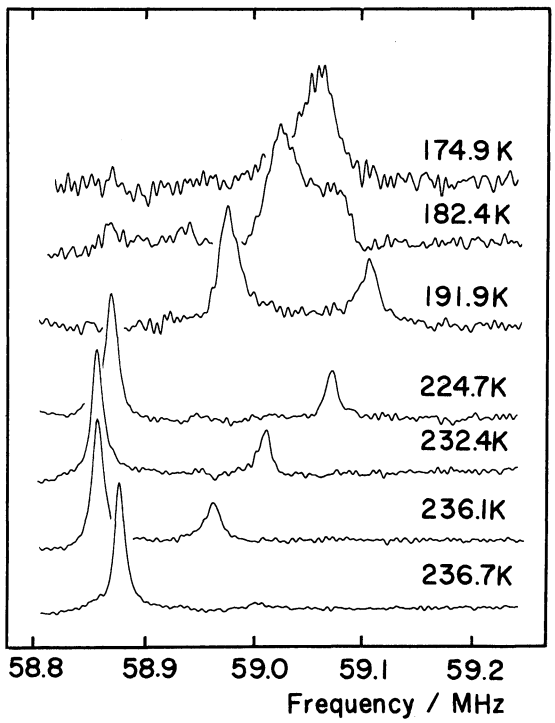

Fig. 5. FT-NQR spectra for $CH_3NH_3PbBr_3$ near β to α phase transition. 100 FID signals were accumulated at a sampling rate of 1 μs before FFT calculations.

determined by DTA measurements. As already stated in our previous paper,[4] the environment around the Sn atom is considerably distorted from the regular $SnBr_6$ octahedron in γ phase, because of an extremely wide distribution of ^{81}Br NQR lines. Unfortunately, however, the structural model for the $SnBr_3^-$ anion in γ phase was not unequivocally deduced. In contrast to the Sn analogue, the splitting of the ^{81}Br NQR lines for the Pb analogue was only slight, suggesting a small distortion of the $PbBr_6$ octahedron from the regular one. This is consistent with the powder X-ray photographs of the low-temperature phases reported by Poglitsch and Weber.[13] Upon cooling $CH_3NH_3PbBr_3$, a single NQR line split into two lines with an intensity ratio of 1:2 at 236.1 K. Upon further cooling, these two lines became broader and showed a decreased intensity, and then, disappeared below 170 K, about 15 degrees above the phase-transition temperature from γ to β phase. The change in the NQR spectra within this temperature range is shown in Fig. 5. The disappearance of the NQR signals below 170 K is probably due to a shortening of the relaxation times, T_1 and T_2^*, with decreasing temperature. For example, the relaxation time at 290 K was 400 μs but at 185 K it decreased to 35 μs, about the same order of the line-width parameter, T_2^*. Below 150 K two strong NQR signals appeared again. In general, with decreasing temperature successive phase transitions are expected for compounds containing $CH_3NH_3^+$ cations, because the effective symmetry of the cation changes from spherical to axial symmetry in the crystal lattice, depending upon the motional state of

the cation.[11] According to our preliminary data regarding the ^{81}Br NQR relaxation times, a drastic decrease in T_1 was observed over a wide temperature range covering the δ–γ–β phase transitions. On the contrary, no detectable anomaly was found at the phase transition from β to α. It is presently not clear what this type NQR relaxation behavior means.

Structural Deformation of the $SnBr_6$ Unit from a Regular Octahedron by Means of ^{119}Sn Mössbauer Spectroscopy. Figure 6 shows the ^{119}Sn Mössbauer spectra at 110 K for a series of $CH_3NH_3Sn_{1-x}Pb_xBr_3$. The profile of the spectra changes from a quadrupole doublet at x=0 to a singlet above x=0.7. Between x=0.2 and 0.6 the spectra were asymmetrical; the spectra were analyzed as a superposition of two components, a quadrupole doublet and a singlet having a relatively high isomer shift (*IS*). The former component was assigned to an Sn site, similar to that found in a $CH_3NH_3SnBr_3$ crystal at 110 K. The latter component increased with increasing x and was assigned to being an Sn atom in a regular octahedral site. These Mössbauer parameters are summarized in Table 2. As stated above, the structural change of the anion is induced by an instability of the symmetric Br–Sn–Br bond. That is, with decreasing temperature an asymmetric Br–Sn···Br bond becomes more stable than that of the symmetric bond. As the result of a deformation of the anion from a regular octahedron, the 5s orbital of the Sn atom contributes to the bond forming sp hybridization. Therefore, a quadrupole splitting having a relatively small isomer shift could be explained semiempirically by the sp hybrid-orbital model.[14,15] If the anion forms a regular octahedron, as in a perovskite lattice, such a large isomer shift as observed in $CsSnBr_3$ (IS=4.0 mm s^{-1}) is expected. Indeed, as Table 2 shows, the ^{119}Sn Mössbauer parameters of $CH_3NH_3SnBr_3$ at 293 K are consistent with this model. On the other hand, a quadrupole doublet (QS=0.5—1.0 mm s^{-1}) having a relatively small isomer shift (IS=3.6—3.8 mm s^{-1}) is expected for an isolated pyramidal anion.[16] A more quantitative treatment is restricted since these parameters strongly depend on the geometry around the Sn atom, such as the bond angle and the bond distance. A series of ^{119}Sn Mössbauer spectra at 110 K and the parameters given in Table 2 show clearly that the $SnBr_6$ unit distorts considerably in the tin-rich region, but remains a regular octahedron above x=0.7 in the perovskite $CH_3NH_3PbBr_3$ matrix. The superimposed spectra between x=0.2 and 0.6 suggest the existence of two phases at 110 K, in contrast to the powder X-ray results at room temperature. This finding suggests that the phase transition, accompanied by a drastic structural change, takes place over a wide temperature range for these solid solutions.

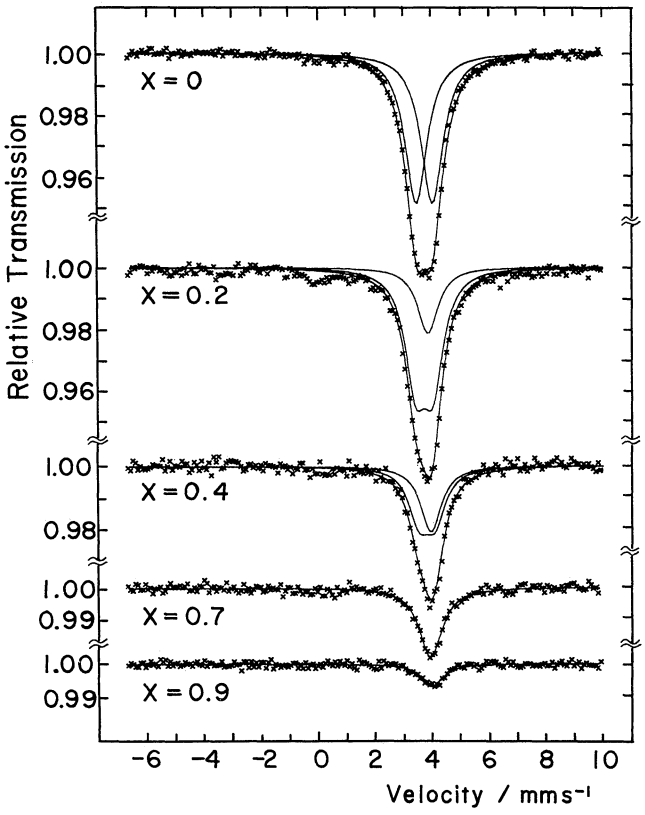

Fig. 6. ^{119}Sn Mössbauer spectra for a series of solid solutions $CH_3NH_3Sn_{1-x}Pb_xBr_3$ at 110 K.

Although many AMX_3 (A=Alkali metal, M=Ge, Sn, Pb, X=halogen) compounds having cubic perovskite structures have been reported in their high-temperature phases,[5,13,18] it is still difficult to predict the structures in their low-temperature phases, since the configuration around the central metal often changes dramatically.

Electrical Conductivity for $CsSnBr_3$ and $CH_3NH_3Sn_{1-x}Pb_xBr_3$. Figure 7 shows plots of the electrical

Table 2. ^{119}Sn Mössbauer Parameters for a Series of Solid Solutions $CH_3NH_3Sn_{1-x}Pb_xBr_3$ at 110 K[a,b]

x	Γ	IS	QS	Relative intensity
	mm/s			
0[c]	0.88(1.05)	3.75(3.98)	0.59(0)	1
0.2	0.88	3.75	0.61	0.76
	0.88	3.88	0	0.24
0.3	0.88	3.74	0.57	0.70
	0.88	3.96	0	0.30
0.4	0.88	3.83	0.57	0.59
	0.88	3.97	0	0.41
0.7	0.98	3.95	0	1
0.9	0.91	4.00	0	1

a) Estimated error ±0.03 mm s^{-1}. b) Line width parameter was fixed to 0.88 mm s^{-1} for x=0—0.4. c) Parameters in parenthesis corresponds to 293 K.

Table 3. Cubic Lattice Constants, Colors, Electrical Conductivity, and Activation Energy for the Electrical Conductivity for $CsSnBr_3$, $CH_3NH_3SnBr_3$, and $CH_3NH_3PbBr_3$

Compound	a/Å	Color		σ/S cm^{-1}	E_a/eV
	295 K	295 K	77 K	295 K	
$CsSnBr_3$	5.808±0.001	Black	Black	4×10[a]	Metallic
$CH_3NH_3SnBr_3$	5.901±0.001	Red	Yellow	2×10^{-5}[b]	0.31
$CH_3NH_3PbBr_3$	5.928±0.002	Orange	Orange	7×10^{-9}[b,c]	0.51

a) Single crystal. b) Pressed powder. c) Extrapolated to 295 K.

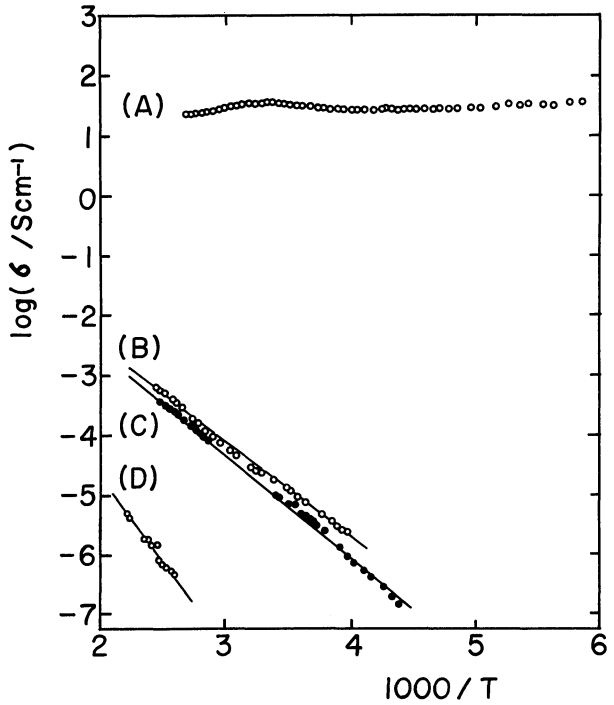

Fig. 7. Temperature dependence of the electrical conductivity for (A) $CsSnBr_3$, (B) $CH_3NH_3SnBr_3$, (C) $CH_3NH_3Sn_{0.5}Pb_{0.5}Br_3$, and (D) $CH_3NH_3PbBr_3$.

conductivity against the inverse temperature for $CsSnBr_3$, $CH_3NH_3SnBr_3$, $CH_3NH_3PbBr_3$, and $CH_3NH_3Sn_{0.5}Pb_{0.5}Br_3$. All of these compounds are isomorphous, with a typical perovskite structure at 293 K. Table 3 summarizes the electrical properties for these compounds, together with the crystal properties. In the replacement of Cs by CH_3NH_3 or Sn by Pb, the conductivity of the perovskite decreased drastically from a metallic-type behavior to a semiconducting type. In these substitutions, the cubic lattice constant, which corresponds to the trans Br–Sn(Pb)–Br bond length, increases slightly. Though phase transitions were reported for $CsSnBr_3$ at 85 and 292 K,[3,13] no observable discontinuity was found regarding the conductivity vs. temperature curve. This suggests that a slight deformation from a cubic perovskite has no singnificant influence on the electronic structure of this compound. In the case of the CH_3NH_3 analogue, however, semiconducting conductivity was observed only for the perovskite phase; no detectable conductivity was found below 229 K. An extremely high electrical conductivity, of the order of of $10—10^3$ S cm^{-1}, was also reported for perovskite $CH_3NH_3SnI_3$ and $CsSnI_3$ (high-temperature phase).[10] The bonding orbitals for a linear –Br–Sn–Br– chain comprise mainly the 4p orbital of the bridging Br atom and the 5p orbital of the Sn atom, and may form both a broadened valence and conduction band due to the infinite chain. The electrical and optical properties of these perovskite may be due to the small band gap between the valence and conduction bands.

References

1) R. G. Gillespie, *J. Chem. Educ.*, **47**, 18 (1970).
2) N. N. Greenwood and A. Earnshaw, "Chemistry of the Elements," Pergamon Press (1984), p. 439.
3) K. Yamada, T. Hayashi, T. Umehara, T. Okuda, and S. Ichiba, *Bull. Chem. Soc. Jpn.*, **60**, 4203 (1987).
4) K. Yamada, S. Nose, T. Umehara, T. Okuda, and S. Ichiba, *Bull. Chem. Soc. Jpn.*, **61**, 4265 (1988).
5) K. Yamada, T. Tsuritani, T. Okuda, and S. Ichiba, *Chem. Lett.*, **1989**, 1325.
6) G. C. Pimentel, *J. Chem. Phys.*, **19**, 446 (1951).
7) J. I. Musher, *Angew. Chem. Int. Ed.*, **8**, 54 (1969).
8) T. A. Albright, J. K. Burdett, and M. H. Whangbo, "Orbital Interactions in Chemistry," John Wiley & Sons, New York (1985), p 258.
9) J. K. Burdett, *Prog. Solid State Chem.*, **13**, 173 (1984).
10) K. Yamada, T. Matsui, T. Tsuritani, T. Okuda, and S. Ichiba, Presented at Xth International Symposium on Nuclear Quadrupole Resonance Spectroscopy, Takayama, Japan, 1989. *Z. Naturforsch.*, **45A**, 307 (1990).
11) Y. Furukawa and D. Nakamura, *Z. Naturforsch.*, **44A**, 1122 (1989).
12) Q. Xu, T. Eguchi, H. Nakamura, N. Nakamura, and M. Kishita, Presented at Xth International Symposium on Nuclear Quadrupole Resonance Spectroscopy, Takayama, Japan, 1989.
13) A. Poglitsch and Weber, *J. Chem. Phys.*, **87**, 6373 (1987).
14) J. D. Donaldson, D. C. Puxley, and M. J. Tricker, *J. Inorg. Nucl. Chem.*, **37**, 655 (1975).
15) E. A. C. Lucken, "Nuclear Quadrupole Coupling Constants," Academic Press, New York (1969).
16) R. V. Parish, "Mössbauer Spectroscopy Application to Inorganic Chemistry," ed by Gray J. Long, Plenum Press, New York (1981), Vol. 1, p. 527.
17) G. Thiele, H. W. Rotter, and K. D. Schmidt, *Z. Anorg. Allg. Chem.*, **559**, 7 (1988).